Striation pattern of target particle and heat fluxes in three dimensional simulations for DIII-D

H. Frerichs, O. Schmitz, D. Reiter, T. E. Evans, and Y. Feng

Citation: Physics of Plasmas **21**, 020702 (2014); doi: 10.1063/1.4864624
View online: http://dx.doi.org/10.1063/1.4864624
View Table of Contents: http://scitation.aip.org/content/aip/journal/pop/21/2?ver=pdfcov
Published by the AIP Publishing

Striation pattern of target particle and heat fluxes in three dimensional simulations for DIII-D

H. Frerichs,[1] O. Schmitz,[1] D. Reiter,[1] T. E. Evans,[2] and Y. Feng[3]
[1]*Institute of Energy and Climate Research—Plasma Physics, Forschungszentrum Jülich GmbH, Association EURATOM-FZJ, Partner in the Trilateral Euregio Cluster, Jülich, Germany*
[2]*General Atomics, P.O. Box 85608, San Diego, California 92186-5608, USA*
[3]*Max-Planck Institute for Plasma Physics, Greifswald, Germany*

(Received 11 December 2013; accepted 27 January 2014; published online 4 February 2014)

The application of resonant magnetic perturbations results in a non-axisymmetric striation pattern of magnetic field lines from the plasma interior which intersect the divertor targets. The impact on related particle and heat fluxes is investigated by three dimensional computer simulations for two different recycling conditions (controlled via neutral gas pumping). It is demonstrated that a mismatch between the particle and heat flux striation pattern (splitting vs. no splitting), as is repeatedly observed in ITER similar shape H-mode plasmas at DIII-D, can be reproduced by the simulations for high recycling conditions at the onset of partial detachment. These results indicate that a detailed knowledge of the particle and energy balance is at least as important for realistic simulations as the consideration of a change in the magnetic field structure by plasma response effects. [http://dx.doi.org/10.1063/1.4864624]

The characterization of particle and heat fluxes to certain wall elements (so called divertor targets) is a key topic for the development of a magnetically confined fusion reactor.[1] One way to control these fluxes is the application of resonant magnetic perturbations (RMPs) at the plasma edge. This method is of particular interest since its recent success in the control of edge localized instabilities (ELMs) found in several present day machines.[2–4] In order to provide reliable predictions of these fluxes, e.g., for the next step fusion device ITER, it is necessary to develop an adequate integrated model.

One candidate for the numerical investigation of particle and heat fluxes in divertor tokamaks under the influence of RMPs is the coupled version of the fluid edge plasma transport code EMC3[5–7] and the kinetic neutral gas transport code EIRENE,[8,9] which has been adapted to divertor tokamaks.[10] Recent simulations for RMP H-mode plasmas at DIII-D have shown a significant striation pattern in both particle and heat fluxes to the divertor target[11] due to the formation of homoclinic tangles,[12,13] however, almost no heat flux striation is observed in the corresponding experiment[14,15] (which is characterized by low collisionality and high triangularity). Other discrepancies between simulations and experiment, such as a strong reduction of the simulated edge temperature by RMPs,[16] could be related to the overestimation of the classical parallel electron heat conductivity at low collisionality.[17] Nevertheless, our first approach to include low collisionality effects in the simulations could not explain the discrepancy in the target heat flux pattern. Another possible mechanism is attributed to a modification of the magnetic field structure by plasma response currents. And although an impact on the striation pattern of the simulated particle and heat fluxes was found[13]—with a slightly stronger decrease of the secondary peaks of the heat flux compared to the particle flux—this effect could not adequately explain the observed discrepancy either.

In the present paper, we study the impact of recycling conditions on the particle and heat flux striation pattern through modeling. The following analysis is based on an ITER similar shape plasma (elongation $\kappa \approx 1.8$ and average triangularity $\delta \approx 0.5$) at the DIII-D tokamak: discharge 132741 at 3760 ms. This discharge is characterized by a plasma current of $I_p = 1.5$ MA and a toroidal magnetic field of $B_t = 1.8$ T at vessel center. The safety factor at 95% of the normalized poloidal flux Ψ_N is $q_{95} = 3.52$. The RMP field is provided by the I-coils (a set of six upper and lower rectangular coils located at the low field side of the machine), which are powered by $I_c = 4$ kA in an even configuration (same current direction in each pair of upper and lower coil) with toroidal base mode number $n = 3$. Error fields and their corrections are neglected at this point, as well as any plasma response effects. The resulting magnetic footprint at the inner strike point (ISP) is visualized in Figure 1 by the penetration of field lines (i.e., particular solutions of the ordinary differential equation (ODE) $\frac{d\mathbf{x}}{dl} = \frac{\mathbf{b}}{|\mathbf{b}|}$, where $\mathbf{b}$ is the vacuum perturbation field superimposed to the equilibrium field).

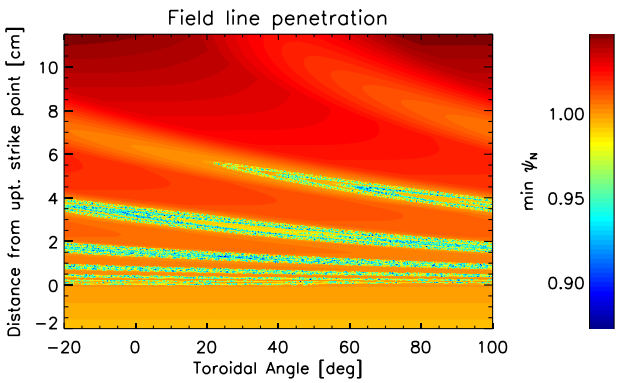

FIG. 1. Modeled magnetic footprint at the inner strike point region depicted by the field line penetration, i.e., minimum of poloidal flux Ψ_N along the corresponding field line.

Boundary conditions for the transport code are the edge input power $P_{\mathrm{ISB}} = 6.3\,\mathrm{MW}$ (i.e., total heating power minus core radiation) and the steady state pumping and re-fueling rate $\Gamma_{\mathrm{in/out}} = 1.1 \times 10^{21}\,\mathrm{s}^{-1}$ based on the corresponding experimental conditions. Impurities are included for diagnostic purposes only, their impact on the main plasma is neglected at this point. Their sources are given by the main ion recycling flux Γ_{rec} and a sputtering coefficient of $c_{\mathrm{sput}} = 1\,\%$. The resulting radiation losses are of the order of $1\% - 2\,\%$ of P_{ISB}. Coefficients for anomalous particle, momentum, and energy cross-field transport are set to $D_{\perp} = 0.2\,\mathrm{m}^2\,\mathrm{s}^{-1}$, $\eta_{\perp} = m_i n_i D_{\perp}$, and $\chi_{e\perp} = \chi_{i\perp} = 0.6\,\mathrm{m}^2\,\mathrm{s}^{-1}$. Literature values for the pumping speed of thermal D_2 at the pump duct entrance are in the range of $30\,\mathrm{m}^3\,\mathrm{s}^{-1}$ to $45\,\mathrm{m}^3\,\mathrm{s}^{-1}$ (see Refs. 18 and 19). The pumping speed L is related to the pump coefficient (see EIRENE documentation[9])

$$L[l/s] = A[\mathrm{cm}^2] \cdot \varepsilon_{\mathrm{pump}} \cdot 3.6838 \sqrt{\frac{T[K]}{m[AMU]}},$$

with an effective pumping area of $A = 2\pi R_{\mathrm{duct}} h_{\mathrm{duct}}$ given by the duct position $R_{\mathrm{duct}} = 142\,\mathrm{cm}$ and height $h_{\mathrm{duct}} = 3.4\,\mathrm{cm}$ as

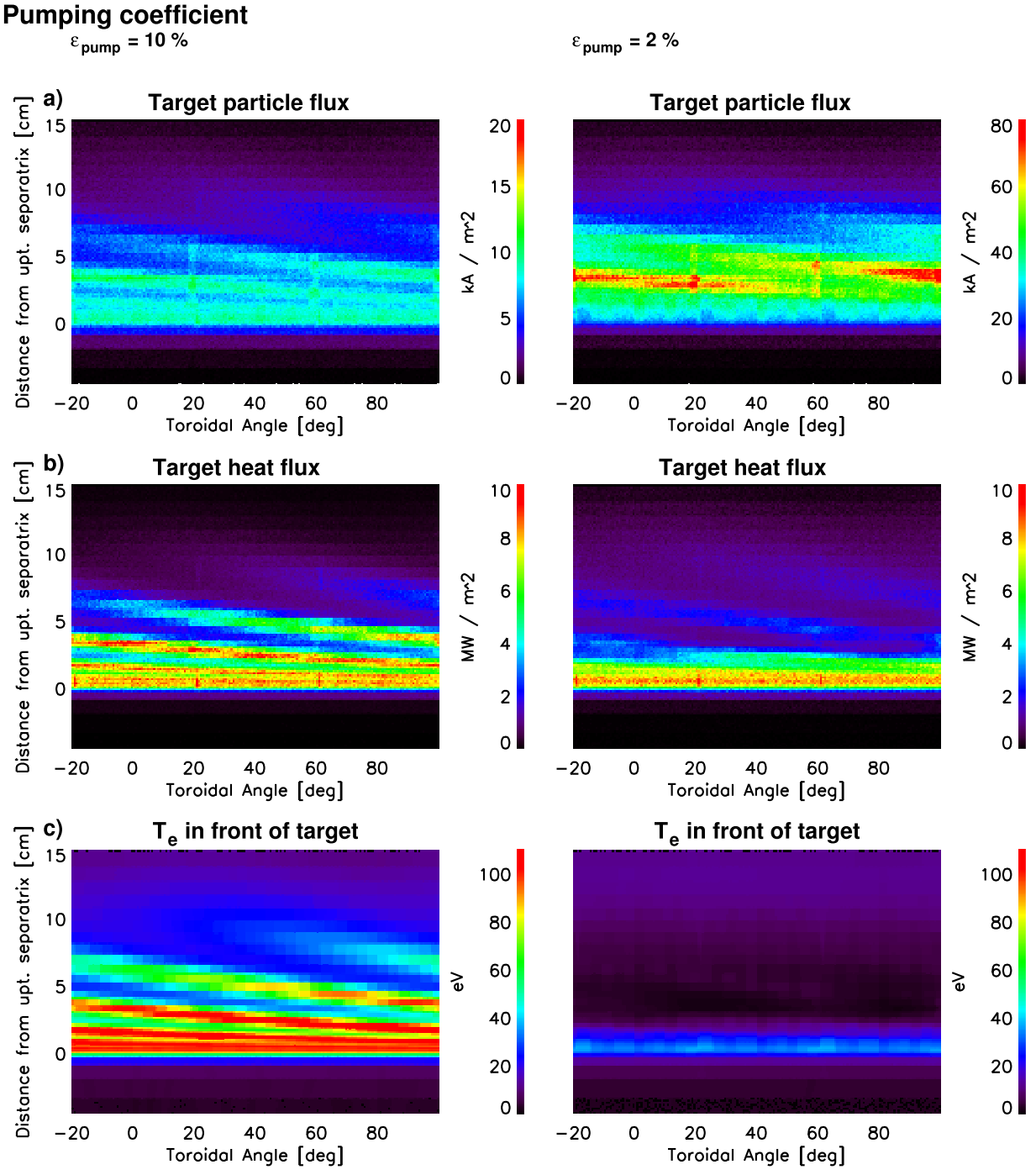

FIG. 2. (a) Target particle flux, (b) target heat flux, and (c) electron temperature in front of the target. Simulation results for the pumping coefficient $\varepsilon_{\mathrm{pump}} = 10\%$ are shown in the left column and those for $\varepsilon_{\mathrm{pump}} = 2\%$ in the right column.

shown in Figure 1 in Ref. 16. The resulting pumping coefficients are in the range of $\varepsilon_{\text{pump}} = 31\% - 46\,\%$ which is consistent with values used in 2D transport modeling[20] with SOLPS5 and is in line with previous estimates.[16] However, a revision of the available experimental data from sweeping the outer strike point during another discharge indicates that the peak recycling flux is rather of the order $500\,\text{kA}\,\text{m}^{-2}$ than the reported $5\,\text{kA}\,\text{m}^{-2}$. This introduces some ambiguity with respect to a reasonable choice for $\varepsilon_{\text{pump}}$ within the given assumptions of the transport model. An easy way to explore such high recycling conditions is to extend our previous study to rather small values for $\varepsilon_{\text{pump}}$. At this point this is a means to control recycling conditions, which could, however, also be affected by adjusting the input/output rate $\Gamma_{\text{in/out}}$, by accounting for gas-puffing in the divertor rather than in the core, or by uncertainties in the power balance (reasons for the latter are discussed below).

A comparison between particle and heat fluxes at the ISP, as well as the temperature in front of the target, are shown in Figure 2 for $\varepsilon_{\text{pump}} = 10\,\%$ (case A) and $\varepsilon_{\text{pump}} = 1.8\,\%$ (case B). It can be seen that a well pronounced striation pattern in both particle and heat fluxes exists for case A (as reported earlier). In order to maintain the given boundary condition $\Gamma_{\text{in/out}}$ for case B, the total amount of recycling Γ_{rec} must increase (but which is still not enough to match the experimental level). As can be seen in Figures 2(a) and 3(a), the relative increase is larger at the outer peaks than at the main strike point (a factor of $\sim$6 at the secondary peak at $\Delta L = 3\,\text{cm}$ compared to a factor of $3 - 3.5$ at the main peak). Nevertheless, a clear "splitting structure" still exists. As a consequence of this strong recycling, the plasma is cooled down to a few eV at the location of the outer peaks. The related heat flux also drops, because the heat conductivity is significantly affected by the temperature change ($\kappa \sim T^{5/2}$), and only the main strike point remains. The particle flux distribution and the low temperature of a few eV at the secondary peak locations indicate that these peaks are in a very high recycling state close to the transition to detachment, while the main peak is still attached.

The shape of the corresponding 1D profile in Figure 3(b) is in good agreement with experimental observations by an IR camera, but the simulated peak level q_{max} far exceeds the experimental one. The reason could either be an overestimation of the edge input power P_{ISB} (because a significant part of the injected power is not coupled to the plasma and lost otherwise), a stronger asymmetry between inner and outer strike point (unfortunately the latter is out of the range of the IR camera for this discharge type), or an underestimation of power loss effects by impurities (e.g., due to a very localized radiation region or by an underestimation of the impurity production rate).

An often used measure for the target particle flux is the observed light emission from neutral hydrogen atoms (H_α line, $\lambda = 656.2\,\text{nm}$) or carbon ions ($C_{II}$ line, $\lambda = 514.3\,\text{nm}$). A virtual camera has been introduced into the simulation code[21] and adapted to DIII-D conditions, which allows to simulate the observed light emission. As can be seen in Figure 3(c), the peak structure in the H_α light is in both cases not as pronounced as in the particle flux. In particular, the primary peak is not present. Nevertheless, the patterns indicate that secondary peaks are present. A trace fluid model[6] has been used to estimate the carbon impurity distribution

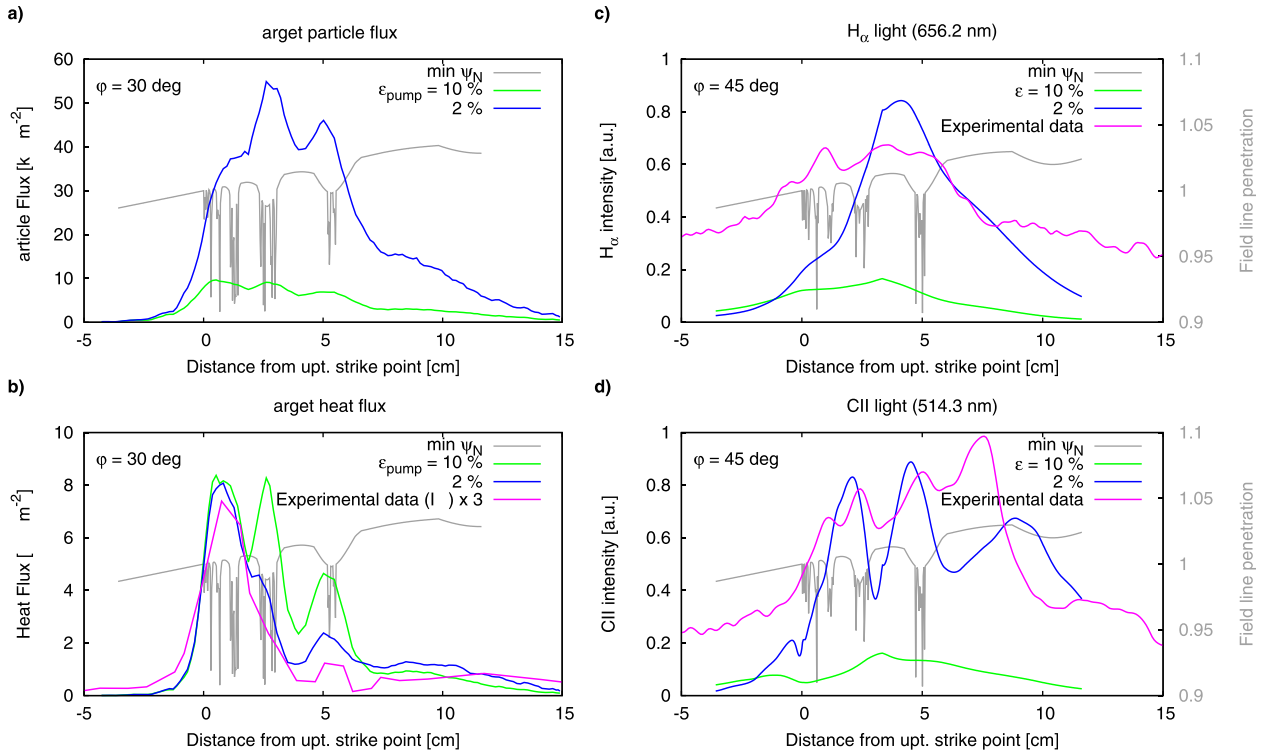

FIG. 3. Profiles of (a) target particle flux, (b) target heat flux, (c) H_α line emission, and (d) C_{II} line emission. Available experimental observations for this discharge (IR, CII) and for a similar discharge (H_α) are given by the magenta profiles and the underlying magnetic configuration is depicted by the gray profiles of the field line penetration.

and to simulate the corresponding C_{II} line emission. A well pronounced striation pattern—as is indeed observed experimentally—can only be observed for case B ($\varepsilon_{pump} \approx 2\%$) as shown in Figure 3(d), although details of the peak structure still differ.

The presented numerical results demonstrate that a discrepancy in the striation pattern of target particle and heat fluxes (i.e., splitting vs. no splitting) can be attributed to recycling conditions. Case B demonstrates that a striation pattern in the magnetic footprint and in the target particle flux can exist even without such evidence in the corresponding target heat flux. However, the mechanism to access these high recycling conditions is not clear at this point. Inconsistencies in the required pumping conditions might be related to the inconsistency between edge input power and peak heat flux at the target, which indicates that additional power loss channels exist, but are missing in the simulations. Nevertheless, these results give a strong indication that a detailed knowledge of the particle and energy balance is at least as important for realistic simulations as the consideration of a change in the magnetic field structure by plasma response effects.

This work is supported in part by the U.S. Department of Energy under DE-FC02-04ER54698.

[1]A. Loarte, B. Lipschultz, A. S. K. an G. F. Matthews, P. C. Stangeby, N. Asakura, G. F. Counsell, G. Federici, A. Kallenbach, K. Krieger, A. Mahdavi, V. Philipps, D. Reiter, J. Roth, J. Strachan, D. Whyte, R. Doerner, T. Eich, W. Fundamenski, A. Herrmann, M. Fenstermacher, P. Ghendrih, M. Groth, A. Kirschner, S. Konoshima, B. LaBombard, P. Lang, A. W. Leonard, P. Monier-Garbet, R. Neu, H. Pacher, B. Pegourie, R. A. Pitts, S. Takamura, J. Terry, E. Tsitrone, and the ITPA Scrape-off Layer and Divertor Physics Topical Group, Nucl. Fusion **47**, S203 (2007).
[2]T. E. Evans, R. A. Moyer, P. R. Thomas, J. G. Watkins, T. H. Osborne, J. A. Boedo, E. J. Doyle, M. E. Fenstermacher, K. H. Finken, R. J. Groebner, M. Groth, J. H. Harris, R. J. L. Haye, C. J. Lasnier, S. Masuzaki, N. Ohyabu, D. G. Pretty, T. L. Rhodes, H. Reimerdes, D. L. Rudakov, M. J. Schaffer, G. Wang, and L. Zeng, Phys. Rev. Lett. **92**(23), 235003 (2004).
[3]Y. Liang, H. R. Koslowski, P. R. Thomas, E. Nardon, B. Alper, P. Andrew, Y. Andrew, G. Arnoux, Y. Baranov, M. Becoulet, M. Beurskens, T. Biewer, M. Bigi, K. Crombe, E. D. L. Luna, P. de Vries, W. Fundamenski, S. Gerasimov, C. Giroud, M. P. Gryaznevich, N. Hawkes, S. Hotchin, D. Howell, S. Jachmich, V. Kiptily, L. Moreira, V. Parail, S. D. Pinches, E. Rachlew, and O. Zimmermann, Phys. Rev. Lett. **98**, 265004 (2007).
[4]W. Suttrop, T. Eich, J. C. Fuchs, S. Günter, A. Janzer, A. Herrmann, A. Kallenbach, P. T. Lang, T. Lunt, M. Maraschek, R. M. McDermott, A. Mlynek, T. Pütterich, M. Rott, T. Vierle, E. Wolfrum, Q. Yu, I. Zammuto, H. Zohm, and A. U. Team, Phys. Rev. Lett. **106**, 225004 (2011).
[5]Y. Feng, F. Sardei, J. Kisslinger, and P. Grigull, J. Nucl. Mater. **241–243**, 930 (1997).
[6]Y. Feng, F. Sardei, P. Grigull, K. McCormick, J. Kisslinger, D. Reiter, and Y. Igitkhanov, Plasma Phys. Controlled Fusion **44**, 611 (2002).
[7]Y. Feng, F. Sardei, J. Kisslinger, P. Grigull, K. McCormick, and D. Reiter, Contrib. Plasma Phys. **44**(1–3), 57 (2004).
[8]D. Reiter, M. Baelmans, and P. Boerner, Fusion Sci. Technol. **47**(2), 172 (2005).
[9]D. Reiter, EIRENE - A Monte Carlo linear transport solver, see http://www.eirene.de.
[10]H. Frerichs, D. Reiter, Y. Feng, and D. Harting, Comput. Phys. Commun. **181**, 61 (2010).
[11]H. Frerichs, D. Reiter, O. Schmitz, T. E. Evans, and Y. Feng, Nucl. Fusion **50**, 034004 (2010).
[12]T. E. Evans, R. K. W. Roeder, J. A. Carter, B. I. Rapoport, M. E. Fenstermacher, and C. J. Lasnier, J. Phys. Conf. Ser. **7**, 174 (2005).
[13]H. Frerichs, D. Reiter, O. Schmitz, P. Cahyna, T. Evans, Y. Feng, and E. Nardon, Phys. Plasmas **19**, 052507 (2012).
[14]O. Schmitz, T. Evans, M. Fenstermacher, H. Frerichs, M. Jakubowski, M. Schaffer, A. Wingen, W. West, N. Brooks, K. Burrell, J. deGrassie, Y. Feng, K. Finken, P. Gohil, M. Groth, I. Joseph, C. Lasnier, M. Lehnen, A. Leonard, S. Mordijck, R. Moyer, A. Nicolai, T. Osborne, D. Reiter, U. Samm, K. Spatschek, H. Stoschus, B. Unterberg, E. Unterberg, J. Watkins, R. Wolf, and the DIII-D and TEXTOR Teams, Plasma Phys. Controlled Fusion **50**, 124029 (2008).
[15]O. Schmitz, T. Evans, M. Fenstermacher, A. McLean, J. Boedo, N. Brooks, H. Frerichs, M. Jakubowski, R. Laengner, C. Lasnier, A. Loarte, R. Moyer, D. Orlov, H. Reimerdes, D. Reiter, U. Samm, H. Stoschus, E. Unterberg, J. Watkins, and the DIII-D and TEXTOR Teams, J. Nucl. Mater. **415**, S886 (2011).
[16]H. Frerichs, D. Reiter, O. Schmitz, D. Harting, T. E. Evans, and Y. Feng, Nucl. Fusion **52**, 054008 (2012).
[17]H. Frerichs, O. Schmitz, D. Reiter, P. Cahyna, Y. Feng, and T. E. Evans, J. Nucl. Mater. **438**, S360 (2013).
[18]R. Maingi, J. G. Watkins, M. Mahdav, and L. Owen, Nucl. Fusion **39**, 1187 (1999).
[19]H. Takenaga, A. Sakasai, H. Kubo, N. Asakura, M. Schaffer, T. Petrie, M. Mahdavi, D. Baker, S. Allen, G. Porter, T. Rognlien, M. Rensink, D. Stotler, and C. Karney, Nucl. Fusion **41**, 1777 (2001).
[20]S. Mordijck, L. Owen, and R. Moyer, Nucl. Fusion **50**, 034006 (2010).
[21]H. Frerichs, D. Reiter, M. Clever, and Y. Feng, In *Proceedings of 37th EPS Conference on Plasma Physics*, P2.127 (2010).